



Nanomedicine: Nanotechnology, Biology, and Medicine 19 (2019) 58–70



nanomedjournal.com

3D Printed scaffolds with hierarchical biomimetic structure for osteochondral regeneration

Xuan Zhou, PhD^a, Timothy Esworthy, MS^a, Se-Jun Lee, BS^a, Shida Miao, PhD^a, Haitao Cui, PhD^a, Michael Plesiniak, PhD^{a,b}, Hicham Fenniri, PhD^c, Thomas Webster, PhD^c, Raj D. Rao, PhD^d, Lijie Grace Zhang, PhD^{a,b,e,f,*}

^aDepartment of Mechanical and Aerospace Engineering, The George Washington University, Washington, DC, USA
 ^bDepartment of Biomedical Engineering, The George Washington University, Washington, DC, USA
 ^cDepartment of Chemical Engineering, Northeastern University, Boston, MA, USA
 ^dDepartment of Orthopedic Surgery, The George Washington University, Washington, DC, USA
 ^cDepartment of Electrical and Computer Engineering, The George Washington University, Washington, DC, USA
 ^fDepartment of Medicine, The George Washington University, Washington, DC, USA
 Revised 24 March 2019

Abstract

Osteochondral defects resulting from trauma and/or pathologic disorders are critical clinical problems. The current approaches still do not yield satisfactory due to insufficient donor sources and potential immunological rejection of implanted tissues. 3D printing technology has shown great promise for fabricating customizable, biomimetic tissue matrices. The purpose of the present study is to investigate 3D printed scaffolds with biomimetic, biphasic structure for osteochondral regeneration. For this purpose, nano-hydroxyapatite and transforming growth factor beta 1 nanoparticles were synthesized and distributed separately into the lower and upper layers of the biphasic scaffold, which was fabricated using 3D stereolithography printer. Our results showed that this scaffold design successfully promoted osteogenic and chondrogenic differentiation of human bone marrow mesenchymal stem cells, as well as enhanced gene expression associated with both osteogenesis and chondrogenesis alike. The finding demonstrated that 3D printed osteochondral scaffolds with biomimetic, biphasic structure are excellent candidates for osteochondral repair and regeneration.

© 2019 Elsevier Inc. All rights reserved.

Key words: 3D printing; Nanomaterials; Osteochondral; Osteogenesis; Chondrogenesis

Osteoarthritis (OA) is the most common form of arthritis and involves cartilage loss, bone degradation, and the development of articular deformities of the hands, knees, hips, and spine. ^{1,2} It has been estimated that as of 2015, about 54.4 million Americans adults have been clinically-diagnosed arthritis with OA. This number is projected to rise to 78.4 million by 2040. ³ Moreover, an estimated 23.7 million Americans suffer from arthritis-attributable limitations to their daily activities. ⁴ In 2013, approximately \$303.5 billion USD, accounting for roughly 1%

of the United States' gross domestic product was attributed to the direct medical costs and indirect loss of income related to OA, with this figure again being projected to increase in the near future.⁵

Currently, the gold standard surgical approach for patients with osteoarthritis is joint replacement with metal or ceramic prosthetic components. Survival of these implants is finite, and the eventual migration of prosthetic components or loosening of implants will frequently result in major loss of tissue, requiring

Conflict of Interest and Disclosure: There are no conflicts to declare.

All sources of support for research: This work was supported by the National Science Foundation Biomedical Engineering program [grant # 1510561] and the George Washington University Center for Microscopy and Image Analysis.

*Corresponding author at: 800 22nd Street NW Science and Engineering Hall, Room 3590, Washington DC, 20052. *E-mail address*: lgzhang@gwu.edu. (L.G. Zhang).

https://doi.org/10.1016/j.nano.2019.04.002

1549-9634/© 2019 Elsevier Inc. All rights reserved.

allograft, autograft, or other synthetic options to fill the defect. Additionally, patients who survive trauma, tumor involvement of bone, or bone and joint infections often have large loss of articular tissue requiring complex reconstructive procedures.^{6,7} Although autograft options are often the best choice for patients, they are usually limited by insufficient donor site bone tissue. Allografts on the other hand rely on donated osteochondral tissue from tissue banks, and are often subject to recipient immunological rejection. Xenografts involve animal tissue donors or artificial tissue, which are also subject to the risk of immunological rejection and technological challenges. 8 Addressing the loss of larger volumes of osteochondral tissue, coupled with the inherently limited regenerative capacity of osteochondral tissue, and the intricacies of articular cartilage composition, makes osteochondral regeneration and reconstruction a significant clinical challenge worldwide.9

Native osteochondral tissue consists of the superficial zone, middle zone, deep zone, calcified zone, and a base of subchondral bone. Generally, the components of osteochondral cartilage are composed of fluid (water and electrolytes, 60–80% wt), extracellular matrix (ECM) (collagen/ proteoglycan, 15–35%wt), and chondrocytes (5% wt). 6,10 Chondrocytes are the only cell type found in articular cartilage and are responsible for the synthesis of ECM components required to maintain the cartilaginous matrix. Unlike self-regenerative bone tissue, the small percentage of chondrocytes embedded in the dense ECM affects both cell mobility and migration. 6 These tissue limitations of articular cartilage are in part why the restoration of the biofunctionality of damaged osteochondral tissues remains a major clinical challenge. Alternative cell sources, such as embryonic stem cells (ESCs)¹¹ and mesenchymal stem cells (MSCs), 9 are considered to be promising cellular approaches for overcoming these restrictions through various tissue engineering strategies. Human bone marrow derived MSCs (hMSCs) are a crucial type of multipotent stem cell of the body and are capable of differentiating into a variety of cell types with specific molecular cues. These cellular fates can include mature osteoblasts, chondrocytes, myocytes, nerve cells, and adipocytes. 9,12 As an example of this molecular guidance of MSC fate assumption, it has been found that transforming growth factor beta1 (TGF-β1) plays a crucial role in regulating and inducing chondrogenic differentiation of MSC and ECM synthesis. 13,14 L-ascorbate acid, β-glycerophosphate and nanocrystalline hydroxyapatite (nHA) are reported to induce osteogenic differentiation of MSCs. 12,15 The multipotency and inducibility properties of hMSCs make them excellent candidates for osteochondral tissue repair.

Over the past few decades, tissue engineering technologies and strategies have also been utilized extensively for tissue repair and regeneration. 9,12 Tissue engineering provides an invaluable platform for tissue regeneration efforts by combining biomimetic matrices and specific cell types in order to generate functional artificial tissue constructs. However, traditional tissue engineering approaches exhibit some critical limitations in their application, such as having low precision and resolution in recapitulating *in vivo* architectures, relying on complex multistep fabricating procedures, and general inefficiency in reestablishing tissue functionality. ¹⁶ Furthermore, traditional tissue engineer-

ing approaches cannot be readily customized to fit the unique structural demands of the tissue defects in each individual patient. In more recent years, the emergence of 3D-printed technologies have greatly enriched and revolutionized conventional tissue engineering approaches. State-of-the-art 3D bioprinting technologies have garnered significant attention in the tissue engineering field because of their capability for fabricating intricate and customizable artificial 3D tissues. In this way, 3D bioprinting technologies can generate high-precision, highefficiency, and customizable matrices with micro-architecture structures using various computer-aided design (CAD) platforms. 9,16 Stereolithography (SL), is a form of 3D printing technology, which utilizes a rapid prototyping lithographic methodology to polymerize photocurable inks in a layer-by-layer fashion through use of specific wave lengths of light. 12,17 In particular, the photocurable inks which can be used in SL printing can be homogenous or heterogenous in composition. Depending on the study purpose, various bioactive molecules, multifunctional nanocomposites, or even live cells can be directly incorporated into the photocurable ink in order to fabricate versatile 3D scaffolds for a number of applications. 9,12,16,17 For our present study, a custom designed table top SL printer which uses a unique photocurable ink was built and prepared in order to fabricate a novel tissue scaffold for osteochondral repair.

Gelatin methacrylate (GelMA) and polyethylene (glycol) diacrylate (PEGDA) were utilized for the preparation of the primary ink (GelMA-PEGDA) in our study. GelMA is a proteinaceous derivative of gelatin which exhibits excellent biocompatibility. Its notable biocompatibility is largely as a function of its abundant arginine-glycine-aspartic acids (RGD) and matrix metalloproteinase (MMP) poly-peptide sequences, which can significantly promote cell attachment and proliferation. 9,12 Meanwhile, another common photocrosslinkable biomaterial, PEGDA, is mixed with GelMA to improve the printability and strength of the scaffolds based our previous experiences. 9,17 nHA has attracted interest as a primary mineral component for the generation of bone-like, hard tissues. nHA has previously been shown by our group to improve osteogenic differentiation of hMSCs and enhance the biomineralization processes. 12,18 Thus, nHA was incorporated into the bioprinted scaffold in order to promote the biomimicry of the subchondral bone of osteochondral tissue. Additionally, TGF-β1 was encapsulated in poly(lactic-co-glycolic acid) nanoparticles (TGF-\beta1 PLGA NPs) for controlled release, to induce chondrogenic differentiation of hMSCs.

The objective of the present study is to create a 3D-printed scaffold with biomimetic biphasic structure for improved osteochondral regeneration. A schematic of the 3D-printed biomimetic structure is shown in Figure 1. Specially, TGF-β1 loaded PLGA nanoparticles were prepared by a co-axial electrospraying method. Utilizing our custom-designed SL-based printer, GelMA-PEGDA-nHA and GelMA-PEGDA-TGF-β1 PLGA nanoparticles were printed in order to generate the subchondral bone and cartilage tissues of the scaffold, respectively. hMSCs were cultured on the osteochondral structures in order to undergo induced osteochondrogenic differentiation. Expression of osteogenetic and chondrogenetic

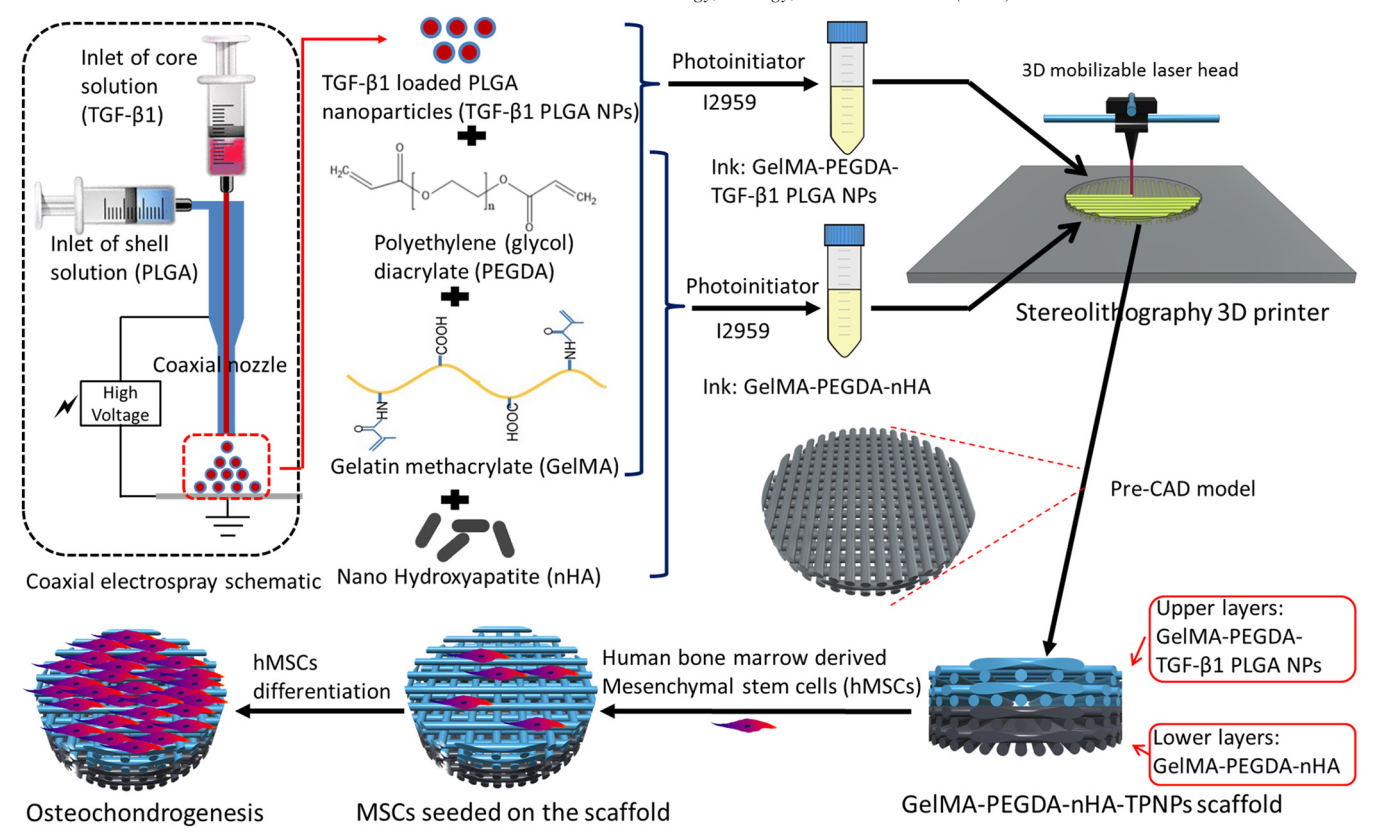


Figure 1. Schematic diagram of a 3D printed osteochondral scaffold.

gene-markers were studied in order to evaluate the differentiation of hMSCs on the 3D scaffolds by means of a real-time quantitative polymerase chain reaction (RT-PCR) assay.

Methods

Preparation of TGF-β1 encapsulated core-shell PLGA NPs

TGF-β1 encapsulated core—shell nanoparticles were prepared *via* a co-axial electrospraying method (Figure 1). The detail processes were described in Supplementary Material.

Synthesis of GelMA and nHA

GelMA was synthesized as described in our previous work. ^{9,12,16,17} The detail processes were described in Supplementary Material.

3D Printed biomimetic osteochondral scaffolds

As aforementioned, the osteochondral scaffolds with biphasic structure consists of subchondral bone and cartilage tissue (Figure 1). The scaffolds were fabricated in a layer-by-layer manner using our table-top SL-based printer using computer aided design (CAD) models. 9,12,16,17 The detail processes were described in Supplementary Material.

Characterization of scaffolds

The morphology of the sample was observed and characterized by transmission electron microscopy (TEM) or scanning electron microscopy (SEM). The mechanical properties of the scaffolds were investigated by unconfined compression testing. The detail processes were described in Supplementary Material.

In vitro TGF-β1 control release study

The encapsulation efficiency (EE%) and drug-loading capacity (LC) were determined by the solvent-extraction method. $^{19-21}$ EE% was defined as the encapsulated protein/ total protein, and LC% was defined as the encapsulated protein/ nanoparticle amount. 20 The TGF- β 1 loaded PLGA nanoparticles with optimal EE% and LC% were chosen for subsequent experimentation. The *in vitro* controlled release of TGF- β 1 from the scaffolds was analyzed in order to investigate the optimal TGF- β 1 concentration. The detail processes were described in Supplementary Material.

hMSC culture

Primary human bone marrow MSCs were harvested from healthy, consenting donors, were distributed, and were thoroughly characterized by the Texas A&M Health Science Center, Institute for Regenerative Medicine. The detail processes were described in Supplementary Material.

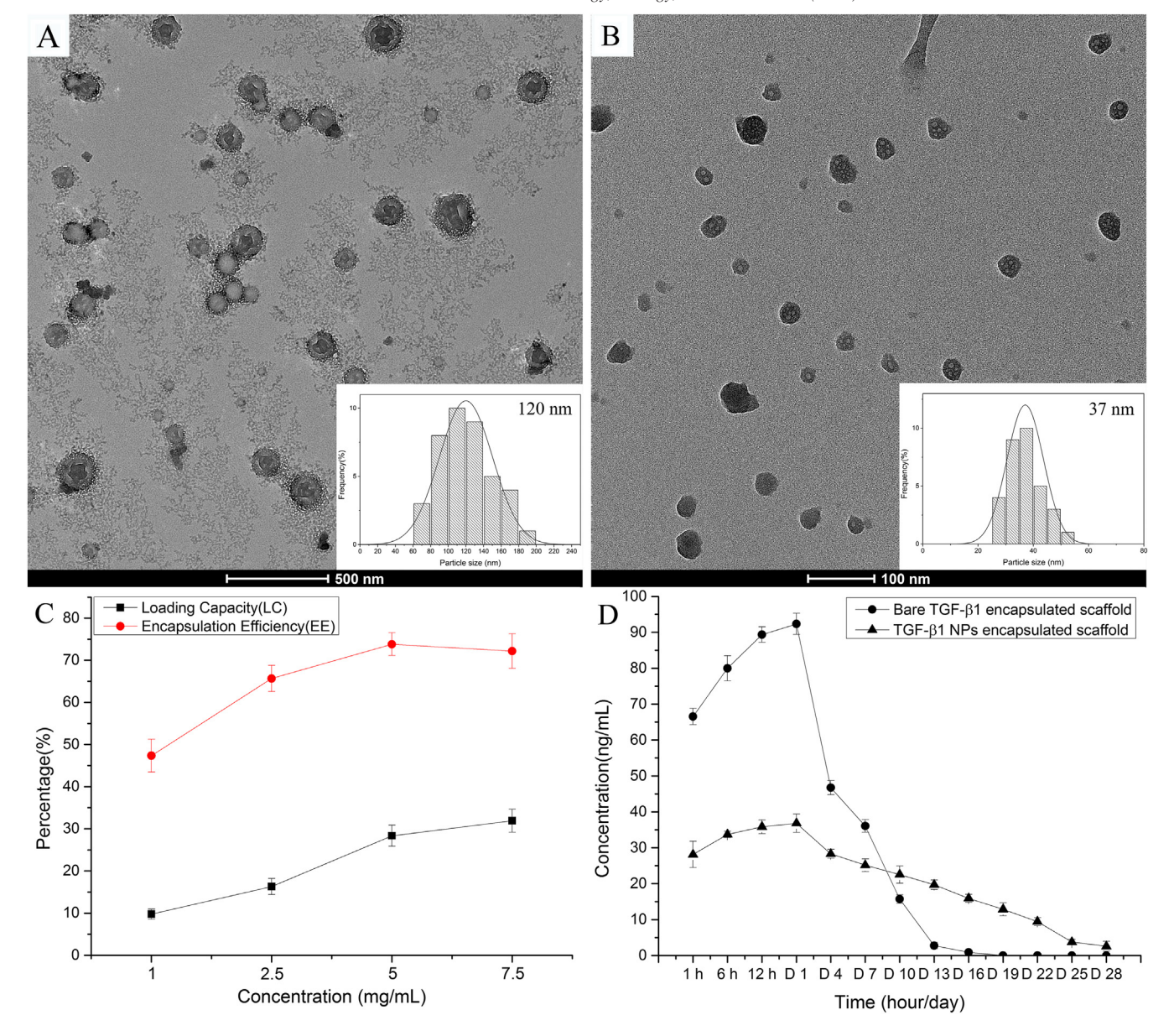


Figure 2. Transmission electron microscopy (TEM) images of (A) TGF- β 1 loaded PLGA NPs and (B) blank PLGA NPs. The inset images display the size distribution of the corresponding nanoparticles. (C) the Loading Capacity (LC) and Encapsulation Efficacy (EE) of TGF- β 1 loaded PLGA NPs at various TGF- β 1 content. (D)The TGF- β 1 released profile from two types of scaffolds (GelMA-PEGDA-TGF- β 1 PLGA NPs and GelMA-PEGDA-bare TGF- β 1).

hMSC proliferation in 3D printed scaffolds

The proliferation of hMSCs on the scaffolds was quantified by CCK-8 method for 6 days. To analyze cell distribution and morphology on the scaffolds, samples were stained with Texas Red-X phalloidin and DAPI. The detail processes were described in Supplementary Material. Once successfully stained, the morphology of hMSCs on the scaffolds was observed by a laser confocal microscope (Carl Zeiss LSM 710).

Osteogenic and chondrogenic differentiation of hMSCs

In order to investigate the importance of incorporating nHA into the osteochondral scaffolds for the guidance of hMSC osteogenic and chondrogenic differentiation, bare scaffolds of

composed of GelMA+PEGDA were employed as a comparative control. hMSCs were induced toward osteogenic and chondrogenic differentiation in order to evaluate the osteochondral potential on each scaffold. The detail processes were described in Supplementary Material. At predetermined time intervals, the scaffolds were rinsed with PBS for histochemical examination.

Histochemical staining was performed after 2 and 4 weeks of culture by Alizarin red-S, Alcian Blue, and Safranin O. 9,22 The detail processes were described in Supplementary Material.

RT-PCR analysis

The expression profiles of osteogenesis-associated (Collagen I, Osteocalcin, OPN, ALP, and Runx-2) and chondrogenesis-

associated (Collagen II a1, Sox-9, and Aggrecan) genes of cells seeded on the various scaffolds were investigated by a real time-PCR assay. The detail processes were described in Supplementary Material. The detailed PCR primer sequences are outlined in Table S1.²³

Statistical analysis

The data presented herein are reported as the mean \pm standard deviation and have been analyzed by a one-way ANOVA method. A P < 0.05 was considered statistically significant in the evaluation of the experimental data.

Results

Characterization of TGF-\(\beta\)1 PLGA NPs

The spherically shaped TGF-β1 loaded PLGA NPs were prepared as outlined in (Figure 2, A). The average sizes of the nanoparticles with and without encapsulated TGF-β1 were about 120 nm and 37 nm, respectively (Figure 2, A and B). These measurements indicate that the particle size increased after loading with TGF- β 1. In order to obtain the optional LC and EE, varying amounts of TGF-β1 were added to optimize the nanoparticles (Figure 2C). The optimal LC% and EE% values were found at a TGF-\(\beta\)1 concentration of 5 mg/mL, and were 28% and 73%, respectively. This concentration of TGF-β1 was chosen for all subsequent experiments. Moreover, the TGF-β1 released from two types of scaffolds (GelMA-PEGDA-TGF-β1 PLGA NPs and GelMA-PEGDA-bare TGF-β1) was investigated for over 4 weeks (Figure 2D). The results illustrated that TGF-β1 concentration in the GelMA-PEGDA-bare TGF-\$1 group increased sharply within 1 day, and decreased with time until it was undetectable at 16 days. Comparatively, TGF-\(\beta\)1 released from GelMA-PEGDA-TGF-\(\beta\)1 PLGA NPs scaffold was sustained over 28 days. This observation could be explained by the fact that the bare TGF-β1 could more easily diffuse from the swelling scaffold into the media solution, which could account for the decrease in observable TGF-β1 over time with the replacement of fresh media every 3 days. Accordingly, the TGFβ1 in GelMA-PEGDA-PLGA NPs was not as easily released, as in the case of these scaffolds, TGF-\beta1 needed to penetrate through both the PLGA shell of the NPs and partition through the matrix network of the scaffolds themselves. We believe that these two barriers in the GelMA-PEGDA-PLGA NP scaffolds contributed significantly to the sustained release of TGF-β1 over the course of 4 weeks.

3D Printed scaffold fabrication and characterization

The study scaffolds with hierarchical structure were successfully fabricated with our customized stereolithography-based 3D printer. SEM images of both the top and bottom views of scaffolds (GelMA-PEGDA-nHA/TGF-β1 PLGA NPs, GelMA-PEGDA-nHA/bare TGF-β1, and GelMA-PEGDA-nHA/blank PLGA NPs) are shown in Figure 3, *A*–*C*. An SEM image illustrating a cross-sectional view of both GelMA-PEGDA-nHA and GelMA-PEGDA-blank PLGA NPs scaffolds is outlined in Figure 3*D*. The uniform pores and channels were arranged in an

orderly distribution throughout the scaffolds. A textural difference between smooth and rough surfaces was observed separately on the upper and lower layers of the scaffolds due to the absence of nHA in the upper layers. Pre-designed CAD models and surface plots of the 3D printed scaffolds are shown in Figures 3 (E, F) and (G, H), respectively. The element analyses of the lower and upper surfaces are shown in Figure 3, *I–K*. The results indicated that the phosphorus and calcium levels of the lower layer were significantly higher than that of upper layer due to the incorporation of nHA [Ca₁₀(PO₄)₆(OH)₂]. The small amounts of phosphorus and calcium detected in upper surface might be associated with phosphate/calcium salt deposition in the PBS solution or/and medium. The compressive modulus of four types of scaffolds is displayed in Fig. S1. Although the compositions are different between the upper layers of the three types of scaffolds, no significant difference was observed among the three groups, which implied that the component difference did not affect the compressive modulus. On the other hand, the compressive modulus of the GelMA-PEGDA control group was significantly lower relative to the other groups because of the absence of nHA in this group.

Proliferation of hMSCs on 3D scaffold

hMSC proliferation on three types of 3D-printed scaffolds was investigated for 6 days (Figure 4A). Confocal microscopy images of hMSCs grown on the scaffold on day 6 were observed, as outlined in Figure 4, *B–D*. hMSCs proliferated considerably well on the three scaffolds over time. The cytoskeleton and cell nuclei of hMSCs were stained and clearly observed on the scaffolds using Texas-Red and DAPI. The F-actin fibers (red stain) stretched and spread along with the scaffolds in three groups. No differences were observed between the three groups.

Evaluation of osteogenic differentiation by gene expression and histological staining

hMSCs are an essential, multipotent form of stem cell which is capable of undergoing both osteogenic and chondrogenic differentiation under specific conditions. In our study, osteogenic differentiation was induced on four types of scaffold for 4 weeks. The expression profiles of the genes (Col I, Osteocacin, OPN, ALP, and Runx-2) were evaluated by RT-PCR analysis (Figure 5). In general, it was found that there was no significant difference between the expression levels of osteogenesis associated genes among the three test groups (GelMA-PEGDA-nHA/TGF-β1 PLGA NPs, GelMA-PEGDA-nHA/bare TGF-β1, and GelMA-PEGDA-nHA/blank PLGA NPs) during each week, but their expression levels were significantly higher than that of GelMA-PEGDA control group at three or 4 weeks (P < 0.05). The expression of the markers Col I, Osteocalcin, and OPN across all groups increased over 4 weeks. Interestingly, after the fourth week of the result, the expression levels of these three genes within the GelMA-PEGDA group were lower than that of the other groups by 19%, 21%, and 26%, respectively. The expression of ALP and Runx-2 increased across all groups for 2 weeks and then decreased. Specifically, the expression of the ALP gene within cells cultured on the GelMA-PEGDA scaffolds was significantly lower than the other groups by 45%

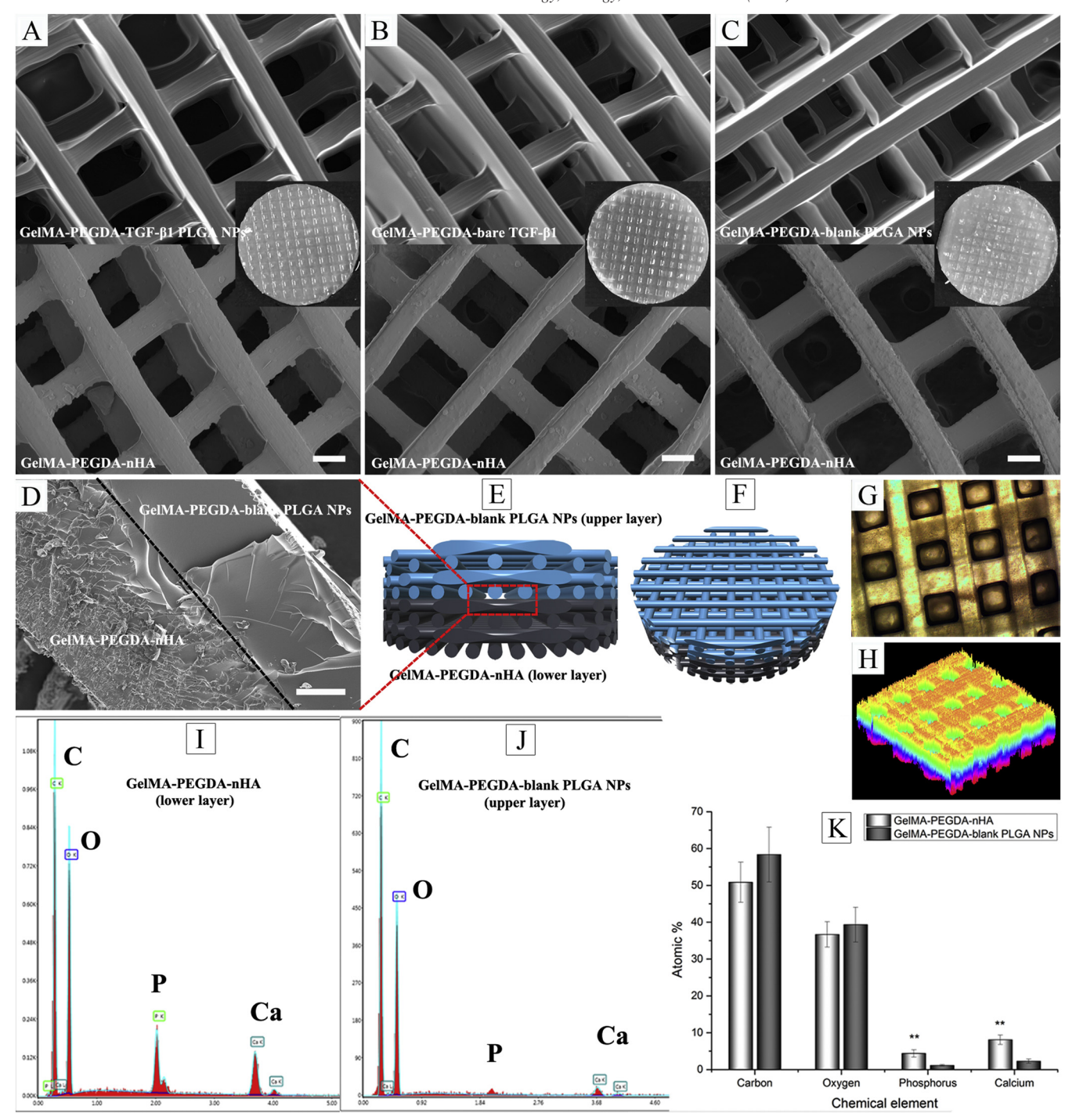


Figure 3. Scanning electron microscopy (SEM) images in top and bottom views of (A) GelMA-PEGDA-nHA/TGF- β 1 PLGA NPs, (B) GelMA-PEGDA-nHA/bare TGF- β 1, and (C) GelMA-PEGDA-nHA/blank PLGA NPs scaffolds. Scale bar = 200 μ m. The inset images are photographs of the corresponding scaffolds. (D) SEM image of cross-sectional view between GelMA-PEGDA-nHA and GelMA-PEGDA-blank PLGA NPs, Scale bar = 100 μ m. (E) Side and (F) top views of the CAD 3D scaffold model. (G) Microscope image and (H) surface plot of 3D printed scaffold. The element analysis (I-J) and the diagram results (K) of lower and upper layers of scaffolds. Data are the mean \pm standard deviation, **P < 0.01 when compared to the upper layer samples.

by the second week. By contrast, the expression of Runx-2 in cells cultured on the GelMA-PEGDA scaffolds increased by 26% compared to the other groups by the second week. The results indicated that hMSCs were successfully induced into

osteogenic differentiation in all groups. Moreover, the presence of TGF- $\beta 1$ in the scaffolds did not appear to influence the osteogenic differentiation of hMSCs, while the incorporation of nHA likely did. As expected, the expression profiles of

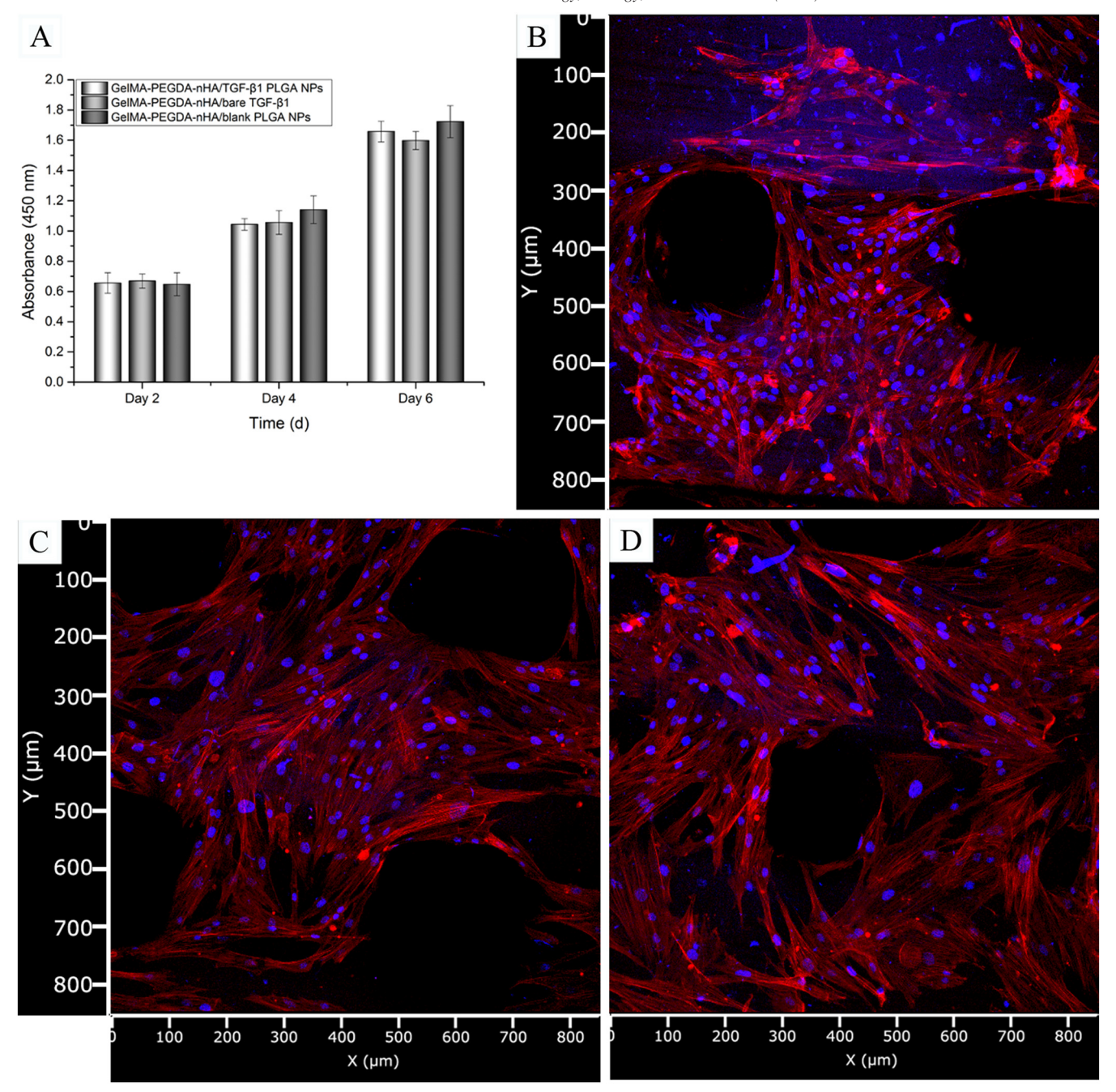


Figure 4. (A) Proliferation (2, 4 and 6 days) and confocal micrographs (Day 6) of hMSCs grown on (B) GelMA-PEGDA-nHA/TGF- β 1 PLGA NPs, (C) GelMA-PEGDA-nHA/bare TGF- β 1, and (D) GelMA-PEGDA-nHA/blank PLGA NPs scaffolds. The cytoskeleton and cell nuclei were stained with Texas Red®-X phalloidin (red) and DAPI (blue), respectively. Data are presented as the mean \pm standard deviation, n=8.

osteogenesis associated genes of cells cultured on the GelMA-PEGDA control scaffolds were lower than that of the other three groups. This observation was attributed to the essential role that nHA plays in improving osteogenesis. 12,17

The gene expression results were further confirmed by histological staining in weeks two and four (Figure 6). Alizarin red S, an anthraquinone dye, has substantial binding affinity to calcium deposition. Therefore, it is typically used to verify the

presence of matrix mineralization, and as such, is considered an early stage marker for osteogenesis. We found that the scaffolds across all groups were stained with a red color at weeks two and four. The stain color in all groups became darker by week 4, suggesting that more calcium is deposited onto the scaffolds over time. There was no discernable difference in staining color among the three test groups (GelMA-PEGDA-nHA/TGF-β1 PLGA NPs, GelMA-PEGDA-nHA/bare TGF-β1, and GelMA-

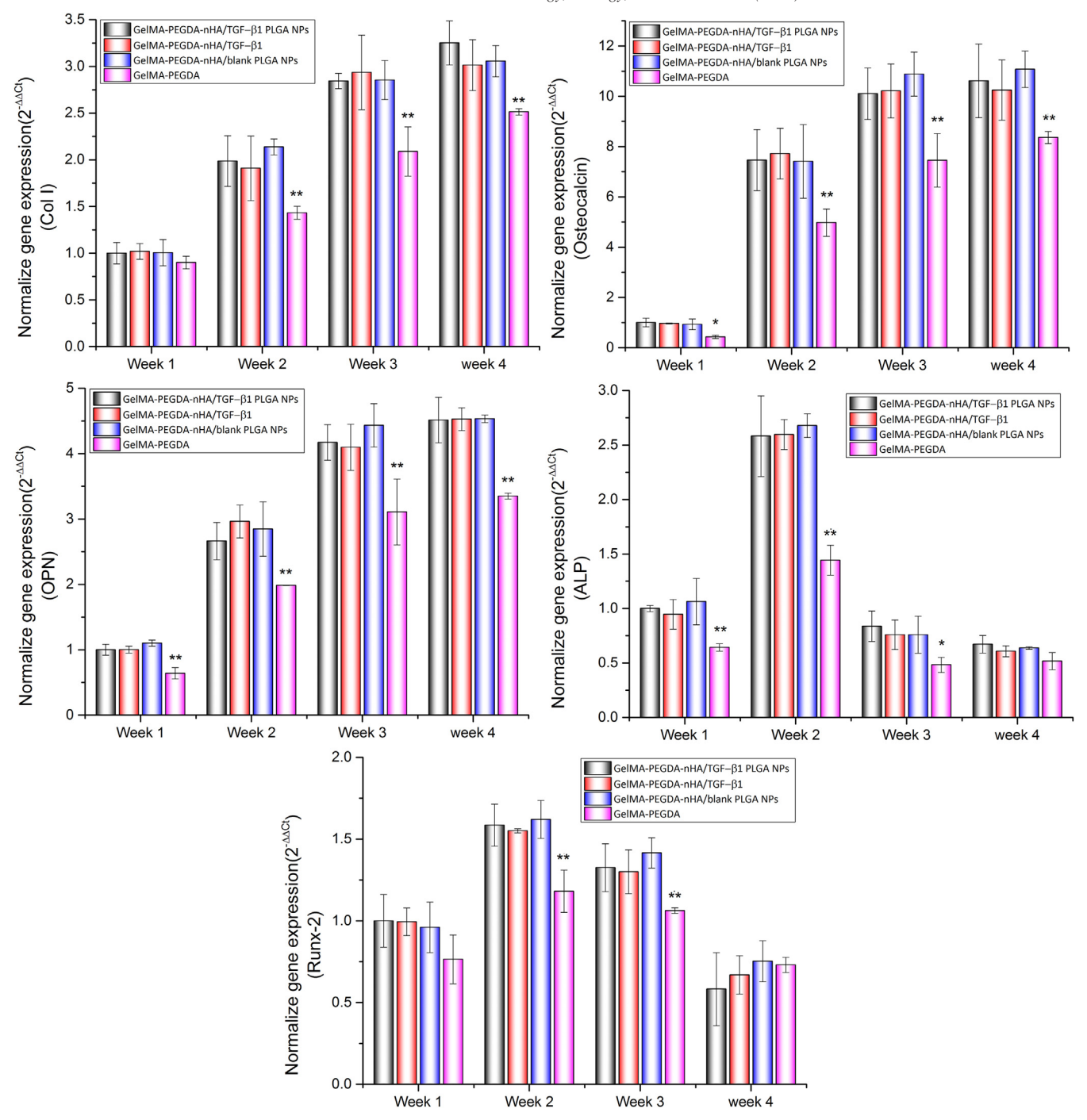


Figure 5. Normalized gene (Col I, Osteocalcin, OPN, ALP, and Runx-2) expressions of hMSCs after osteogenic differentiation on various scaffolds over 4 weeks. Data are the mean \pm standard deviation, n = 8. *P < 0.05 and **P < 0.01 when compared to all other groups at each time point.

PEGDA-nHA/blank PLGA NPs) during each week, but all three showed deeper staining color than that of the GelMA-PEGDA group at each subsequent time point. This observation demonstrates that greater mineralization was generated by these three groups of scaffolds when compared to the GelMA-PEGDA control group. These results are consistent with the osteogenic gene expression profiles that we observed, indicating

that the 3D-printed biomimetic, biphasic osteochondral scaffolds provide a platform for hMSCs growth and osteogenesis.

Evaluation of chondrogenic differentiation by gene expression and histological staining

To further evaluate the 3D-printed biomimetic, biphasic scaffolds, chondrogenic differentiation was induced on four

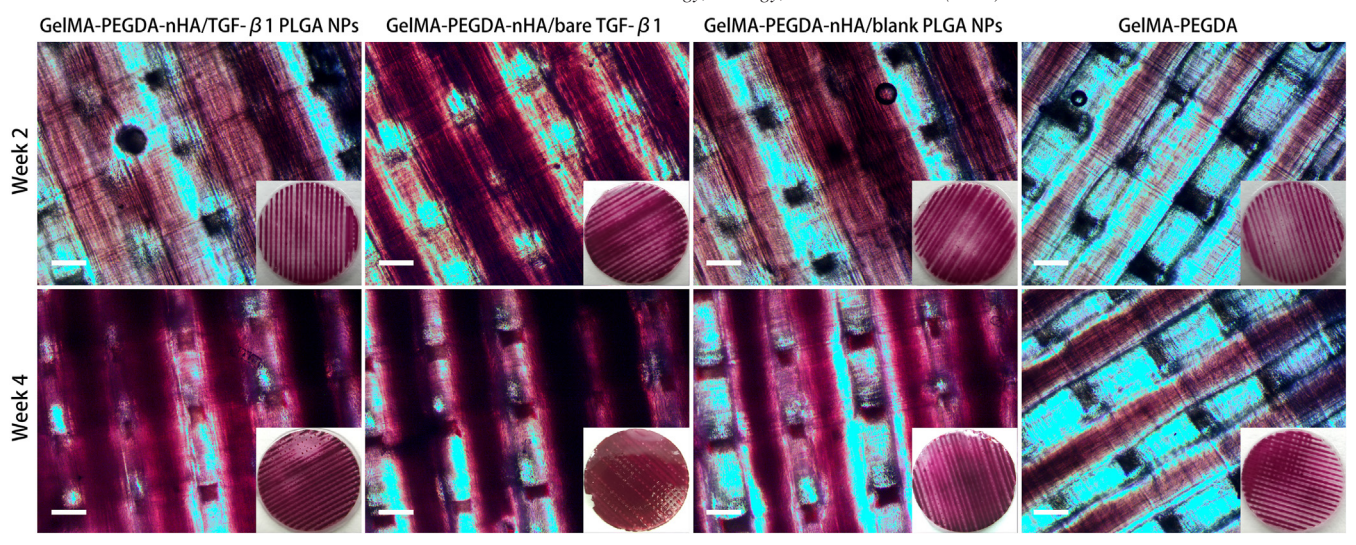


Figure 6. Light microscopy images of Alizarin red S stained hMSCs after osteogenic differentiation on the surface of the scaffolds with different components at weeks 2 and 4. Scale bar = $200 \mu m$.

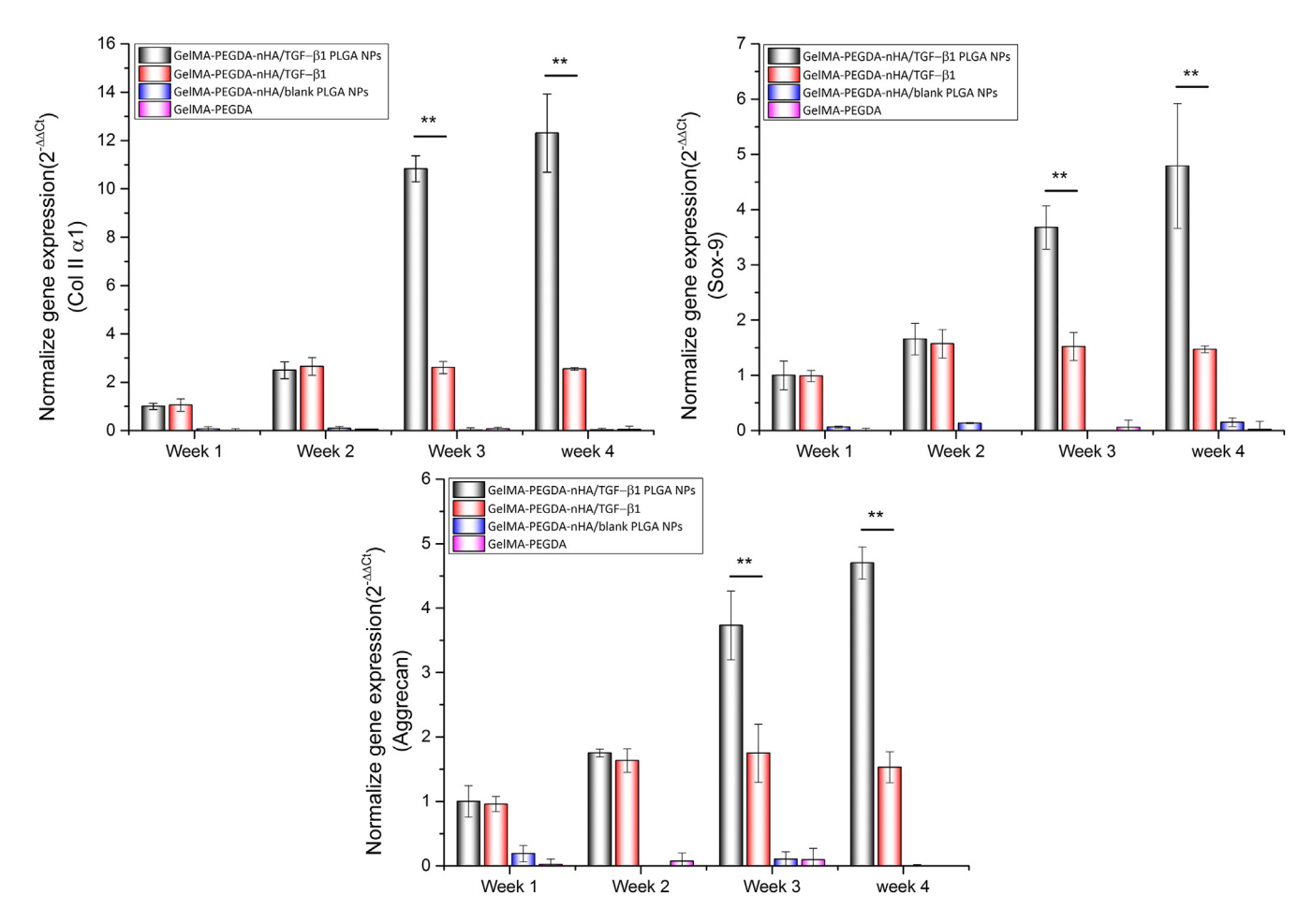


Figure 7. Normalized gene expression (Col II α 1, Sox-9, and Aggrecan) of hMSCs after chondrogenic differentiation on various scaffolds over 4 weeks. Data are presented as the mean \pm standard deviation, n = 8. **P < 0.01 when compared to all other groups at each time point.

types of scaffold for 4 weeks. The expression profiles of the genes (Col II, SOX-9, and Aggrecan) were evaluated by RT-PCR analysis (Figure 7). Interestingly, these three chondrogen-

esis associated genes were not expressed in two groups (GelMA-PEGDA-nHA/blank PLGA NPs and GelMA-PEGDA) within 4 weeks. These results suggest that TGF-β1 was depleted in these

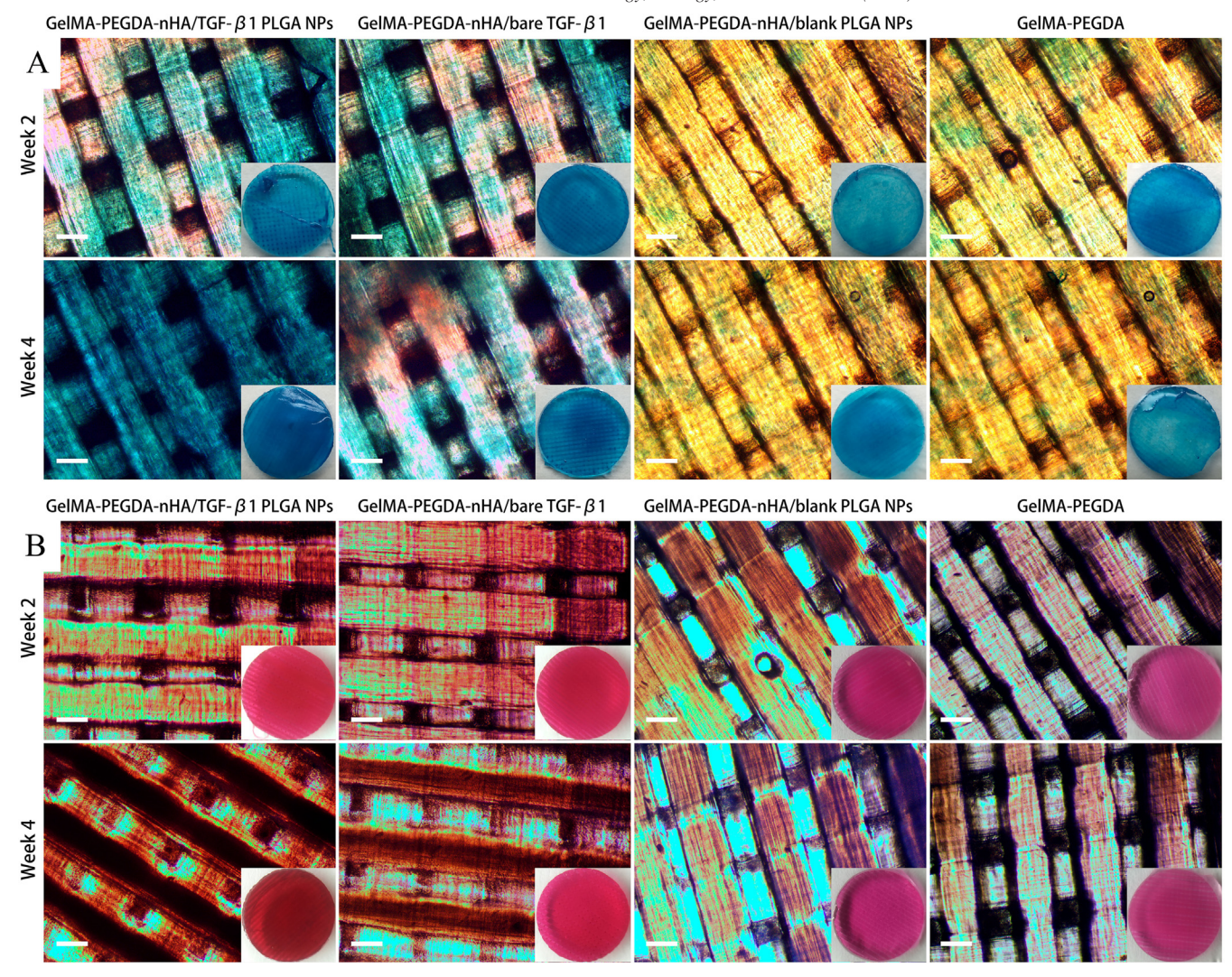


Figure 8. Light microscopy images of (A) Alcian Blue and (B) Safranin O stained hMSCs after chondrogenic differentiation on the surface of the scaffolds with different components at weeks 2 and 4. Scale bar = 200 µm.

scaffolds, which was also not present in the culture media. These observations strongly suggest that TGF-β1 is a crucial factor for chondrogenesis. The expression profiles of the chondrogenic genes of cells cultured on the GelMA-PEGDA-nHA/TGF-\(\beta\)1 PLGA NPs scaffolds increased over 4 weeks, while that of the cells on the GelMA-PEGDA-nHA/bare TGF-\(\beta\)1 scaffolds only increased over 2 weeks and then plateaued. Moreover, the expression of the target genes (Col II, SOX-9, and Aggrecan) in the former group was significantly higher than that of the latter groups by 383%, 225%, and 206% after the fourth week, respectively (P < 0.01). These results indicated that the chondrogenic differentiation of cells cultured on the GelMA-PEGDA-nHA/TGF-β1 PLGA NPs scaffolds was substantially induced for 4 weeks whereas chondrogenic differentiation of hMSCs on the GelMA-PEGDA-nHA/bare TGF-β1 scaffolds was induced for only 2 weeks.

Histological analysis at study weeks two and four were carried out to further evaluate downstream effects of

chondrogenesis-associated gene expression (Figure 8). Alcian Blue is typically used to stain acidic polysaccharides, such as glycosaminoglycans (GAG), in cartilage and other extracellular matrices. 9 Safranin O is a cationic dye also used for staining proteoglycans and GAG in cartilage. 24 The colors in two groups of (GelMA-PEGDA-nHA/TGF-\beta1 PLGA NPs, and GelMA-PEGDA-nHA/bare TGF-β1) were blue or blue-green and became more pronounced over time. Meanwhile, the blue stain color was minimally observed in two of the test groups (GelMA-PEGDA-nHA/blank PLGA NPs and GelMA-PEGDA) across the two time points. These results indicate that chondrogenic differentiation was induced in the scaffolds with TGF-\beta1 incorporation groups; whereas it was not induced in the scaffolds without TGF-β1 incorporation (the latter two groups). Furthermore, the staining color in the GelMA-PEGDA-nHA/TGF-β1 PLGA NPs group was deeper when compared to the other groups at week four. This observation likely implies that more GAG was synthesized on the scaffold with TGF-β1 NPs than that with bare TGF-β1 after chondrogenic differentiation was induced over a period of 4 weeks. This observation is highly consistent with the results of the gene expression analysis. Additionally, the same trend appeared during the histological staining with Safranin O (Figure 8*B*). Moreover, more proteoglycans and GAG were synthesized on the scaffolds containing TGF-β1NPs in comparison with bare TGF-β1, likely as a function of the sustained release TGF-β1 over the course of 4 weeks in former scaffold. This observation could also be explained by the fact that TGF-β1 played an essential role in the induction of hMSC chondrogenic differentiation. These results have demonstrated that the 3D-printed biomimetic, biphasic osteochondral scaffolds (GelMA-PEGDA-nHA/TGF-β1 PLGA NPs) are valuable candidates for use in both bone and cartilage induction for relevant clinical applications.

Discussion

Preparation of biphasic scaffolds

In our study, TGF- β 1 loaded PLGA NPs with 120 nm particle size (Figure 2) were prepared using co-axial electrospraying. GelMA and nHA were successfully synthesized by chemical modification and hydrothermal methods, respectively. GelMA-PEGDA was employed as an elementary ink for this study. Finally, nHA and TGF- β 1 PLGA NPs were distributed separately into discrete lower and upper layers for our biomimetic, biphasic scaffolds (GelMA-PEGDA-nHA/TGF- β 1 PLGA NPs) using our stereolithography-based 3D printer. The biphasic scaffolds with uniform pores and channels display a smooth upper surface and rough lower surface due to nHA incorporation in the lower layer (Figure 3). The biphasic scaffold can steadily release TGF- β 1 for as long as 4 weeks, as opposed to the scaffolds with bare TGF- β 1 which released the factor within 2 weeks (Figure 2).

MSCs proliferation on scaffolds

hMSCs grew well over time on the scaffolds and no growth differences were noted within a period of 6 days, with or without TGF-β1 incorporation (Figure 4). Our results imply that TGF-β1 does not affect hMSCs proliferation. TGF-β1 is a multifunctional cytokine that regulates various biological processes, including cell differentiation, apoptosis, immunity, and the production of the ECM. ^{25,26} The regulatory effects of TGF-β1 on cell proliferation is not as certain, and may vary depending on different cell type. TGF-\(\beta\)1 has been reported to inhibit proliferation of most cell types, including epithelial, endothelial, hematopoietic cells, and embryonic fibroblasts.²⁷ Although some reports claim that MSC proliferation could be promoted by TGF-β1, ^{25,28,29} other studies have shown that TGF-β1 will not induce MSC growth, but rather works to sustain cell survival, $^{30-32}$ or even inhibit MSC growth at high TGF- $\beta 1$ concentrations. 33,34 As such, the role that TGF- $\beta 1$ plays in cellular proliferation and survival remains a matter of significant debate. In our study, we found that there were no significant differences in cell growth between the three groups tested. These findings imply that TGF-β1 does not affect the proliferation of hMSCs in 6 days of continuous culturing carried out in our study.

Osteogenesis on scaffold

The osteogenenic differentiation of hMSCs was induced as expected on the scaffolds, and there were no differences in these scaffolds with or without TGF- β 1 incorporation (Figure 5). However, osteogenic differentiation was more pronounced in scaffolds which had nHA incorporated compared to scaffolds that did not. Specifically, the expression of osteogenesis associated genes Col I, Osteocalcin, and OPN increased over time, while the gene expression of ALP and Runx-2 increased over 2 weeks and then decreased. The results were confirmed by the histological staining with Alizarin red S, indicating calcific deposition and matrix mineralization (Figure 6).

The Col-I gene is associated with the synthesis and secretion of collagen type I, which plays an important role in the formation of bone tissue. The collagen type I fiber is an essential organic component of the ECM in bone tissue and plays a crucial role in bone restructuring. 6 Meanwhile, the Osteocalcin gene encodes an essential bone protein produced by osteoblasts, also known as the bone gamma-carboxyglutamic acid-containing protein (BGLAP), which has a high binding affinity to calcium and hydroxyapatite. The Osteocalcin gene is considered to be the primary biomarker for bone remodeling and rebuilding.³⁵ The Osteopontin (OPN) gene encodes the Secreted Phosphoprotein 1 (SPP1), which in turn also has a high binding affinity for hydroxyapatite. 35 Both Osteocalcin and OPN are associated with calcium deposition and are involved in bone matrix mineralization. Alkaline phosphatase (ALP) in bone tissue is encoded by the tissue non-specific ALP (TNAP) gene, and is regarded as a byproduct of osteoblast activity. 36 It is expressed early in the initial phases of bone development and is up-regulated during the active formation of new bone. Conversely, the expression of ALP decreases as bone tissue matures. Therefore, ALP is considered to be an early marker of osteogenic mineralization. Runt-associated transcription factor 2 (Runx2) is also an early marker, and a key transcription factor associated with osteoblast differentiation. The Runx2 gene was reported to be detectable in pre-osteoblasts and up-regulated in immature osteoblasts, but ultimately down-regulated during osteoblast maturation.³⁷ In the current study, the three types of scaffolds (GelMA-PEGDAnHA/TGF-β1 PLGA NPs, GelMA-PEGDA-nHA/bare TGF-β1, and GelMA-PEGDA-nHA/blank PLGA NPs) differed in the composition of their upper layers, but showed no difference in osteogenesis. Meanwhile, the effects of nHA on osteogenesis was found to be much greater than that of TGF-β1. The results suggest that scaffolds with or without incorporated TGF-β1 will likely not influence the osteogenic differentiation of hMSCs.

As mentioned above, TGF- $\beta 1$ is a multifunctional cytokine which is believed to be involved in regulating multiple biological processes, including cell differentiation, apoptosis, immunity, and the production of the ECM. ^{25,26} However, there have been several debatable reports on the effects of TGF- $\beta 1$ on the osteogenic differentiation of MSCs. ²⁴ Li, ³² Tang, ³⁸ and Zhao ³⁹ have reported that TGF- $\beta 1$ has a positive effect on the osteogenic differentiation of MSCs, and plays a crucial role in bone formation and resorption. Lieb ⁴⁰ and Liu ⁴¹ revealed a dual effect of TGF- $\beta 1$, which promoted osteogenic differentiation at low concentrations (0.1–1 ng/mL) and inhibited it at high

concentration (10 ng/mL). According to Labour³¹ and Jian,⁴² TGF-β1 has a negative effect on osteogenesis, which may be associated with the down-regulation of the catenin/Smad3-mediated signaling pathway. In this study, our results demonstrated that osteogenesis is not notably affected by TGF-β1, and that osteogenic differentiation appears to be more impacted by the presence of nHA. Overall, we found that the osteogenic differentiation of hMSCs is mediated primarily by other various experimental conditions, such as cell density, and additional molecular components of the osteogenic media.

Chondrogenesis on scaffold

Furthermore, the chondrogenic differentiation of hMSCs was also expectedly higher on the scaffolds with incorporated TGF- $\beta1$ PLGA NPs than those with incorporated bare TGF- $\beta1$ (Figure 7). This was likely a function of the longer period of TGF- $\beta1$ release from the former scaffold. Chondrogenesis was not observed on the scaffolds without TGF- $\beta1$ incorporation. These results suggest that TGF- $\beta1$ plays a crucial role in the chondrogenic differentiation of hMSCs. Specifically, the expression of the chondrogenesis-associated genes Col II, SOX-9, and Aggrecan increased over time in the scaffolds with TGF- $\beta1$ PLGA NPs incorporation, and was notably higher than that of scaffolds which incorporated bare TGF- $\beta1$ alone. Interestingly, these three genes were not significantly expressed in scaffolds that did not incorporate TGF- $\beta1$.

These observations were readily associated with TGF-β1 release profiles: TGF-β1 released from GelMA-PEGDA-TGF-β1 PLGA NPs scaffold could be sustained for almost 4 weeks, but only for 2 weeks in the GelMA-PEGDA-nHA/bare TGF-β1 scaffolds. Collagen Type II is the major component of articular cartilage⁶ Aggrecan and proteoglycan are the primary extracellular matrix (ECM) components in hyaline cartilage, and provide compressive properties to the tissue. 9 The SOX-9 gene is usually expressed in chondrocytes and cartilage relevant tissues, and is synchronously co-expressed with Collagen Type II. 43,44 The combined expression of these genes is highly relevant to the production of cartilage ECM. In our current work, the Real-Time PCR results illustrated that the 3D-printed biomimetic, biphasic osteochondral GelMA-PEGDA-TGF-β1 PLGA NPs scaffold is a very viable substrate for the promotion of chondrogenesis. Comparatively, TGF-β1 has been reported and verified widely to be a potent chondrogenic inducer of hMSCs. Our results further confirm the function of TGF-\(\beta\)1 in promoting chondrogenic differentiation. These results were confirmed by the histological staining of Alcian Blue and Safranin O, which indicate GAG and ECM synthesis (Figure 8).

In summary, our results demonstrate that 3D-printed osteochondral scaffolds with biomimetic, biphasic structure are excellent substrates for promoting osteogenesis and chondrogenesis, and exhibit great promise for future applications in bone and cartilage repair and regeneration.

Appendix A. Supplementary data

Supplementary data to this article can be found online at https://doi.org/10.1016/j.nano.2019.04.002.

References

- Nowicki MA, Castro NJ, Plesniak MW, Zhang LG. 3D printing of novel osteochondral scaffolds with graded microstructure. *Nanotechnology* 2016:27414001.
- Castro NJ, O'Brien J, Zhang LG. Integrating biologically inspired nanomaterials and table-top stereolithography for 3D printed biomimetic osteochondral scaffolds. *Nanoscale* 2015;7:14010-22.
- Barbour KE, Helmick CG, Boring M, Brady TJ. Vital signs: prevalence of doctor-diagnosed arthritis and arthritis-attributable activity limitation-United States, 2013-2015. Morb Mortal Wkly Rep 2017;66:246-53.
- Boring MA, Hootman JM, L Y, Theis KA, Murphy LB, Barbour KE, et al. Prevalence of arthritis and arthritis-attributable activity limitation by urban-Rural County classification -United States, 2015. *Morb Mortal* Wkly Rep 2017;66:527-32.
- 5. Yelin E, Weinstein S, King T. The burden of musculoskeletal diseases in the United States. *Semin Arthritis Rheum* 2016;**46**(3):259-60.
- Zhang L, Hu J, Athanasiou KA. The role of tissue engineering in articular cartilage repair and regeneration. Crit Rev Bioeng 2009;37:1-57
- Castro NJ, Patel R, Zhang LG. Design of a novel 3D printed bioactive nanocomposite scaffold for improved osteochondral regeneration. *Cellular and molecular bioengineering* 2015;8:416-32.
- Chu CR, Szczodry M, Bruno S. Animal models for cartilage regeneration and repair. Rev 2010;16:105-15.
- Zhou X, Nowicki M, Cui H, Zhu W, Fang X, Miao S, et al. 3D bioprinted graphene oxide-incorporated matrix for promoting chondrogenic differentiation of human bone marrow mesenchymal stem cells. *Car*bon 2017:116:615-24.
- Nowicki M, Castro NJ, Rao R, Plesniak M, Zhang LG. Integrating threedimensional printing and nanotechnology for musculoskeletal regeneration. *Nanotechnology* 2017;28382001.
- Toh WS, Lee EH, Guo X-M, Chan JKY, Yeow CH, Choo AB, et al. Cartilage repair using hyaluronan hydrogel-encapsulated human embryonic stem cell-derived chondrogenic cells. *Biomaterials* 2010;31:6968-80.
- Zhou X, Castro NJ, Zhu W, Cui H, Aliabouzar M, Sarkar K, et al. Improved human bone marrow mesenchymal stem cell osteogenesis in 3D bioprinted tissue scaffolds with low intensity pulsed ultrasound stimulation. Sci Rep 2016;632876.
- Joyce ME, Roberts AB, Sporn MB, Bolander ME. Transforming growth factor-beta and the initiation of chondrogenesis and osteogenesis in the rat femur. J Cell Biol 1990;110:2195-207.
- Worster AA, Nixon AJ, Brower-Toland BD, Williams J. Effect of transforming growth factor beta1 on chondrogenic differentiation of cultured equine mesenchymal stem cells. Vet Res 2000;61:1003-10.
- Thibault RA, Scott Baggett L, Mikos AG, Kasper FK. Osteogenic differentiation of mesenchymal stem cells on Pregenerated extracellular matrix scaffolds in the absence of osteogenic cell culture supplements. *Tissue Eng Part A* 2010;16:431-40.
- Zhou X, Cui H, Nowicki M, Miao S, Lee SJ, Masood F, et al. Threedimensional-bioprinted dopamine-based matrix for promoting neural regeneration. ACS Appl Mater Interfaces 2018;10:8993-9001.
- Zhou X, Zhu W, Nowicki M, Miao S, Cui H, Holmes B, et al. 3D bioprinting a cell-laden bone matrix for breast Cancer metastasis study. ACS Appl Mater Interfaces 2016;8:30017-26.
- Zhang L, Chen Y, Rodriguez J, Fenniri H, Webster TJ. Biomimetic helical rosette nanotubes and nanocrystalline hydroxyapatite coatings on titanium for improving orthopedic implants. *Nanomedicine* 2008;3:323-34.
- Zhou X, Kong M, Cheng X, Li J, Li J, Chen X. Investigation of acetylated chitosan microspheres as potential chemoembolic agents. *Biointerfaces* 2014;123:387-94.
- Zhou X, Kong M, Cheng XJ, Feng C, Li J, Li JJ, et al. In vitro and in vivo evaluation of chitosan microspheres with different deacetylation degree as potential embolic agent. *Carbohydr Polym* 2014;113:304-13.

- Li J, Kong M, Cheng XJ, Dang QF, Zhou X, Wei YN, et al. Preparation of biocompatible chitosan grafted poly(lactic acid) nanoparticles. *Biol Macromol* 2012;51:221-7.
- Delorme B, Charbord P. Culture and characterization of human bone marrow mesenchymal stem cells. *Methods Mol Med* 2007;140:67-81.
- Zhou J, Xu C, Wu G, Cao X, Zhang L, Zhai Z, et al. In vitro generation of osteochondral differentiation of human marrow mesenchymal stem cells in novel collagen-hydroxyapatite layered scaffolds. *Acta Biomater* 2011;7:3999-4006.
- Zhao L, Hantash BM. TGF-beta1 regulates differentiation of bone marrow mesenchymal stem cells. *Vitam Horm* 2011;87:127-41.
- Massague J, Blain SW, Lo RS. TGFbeta signaling in growth control, cancer, and heritable disorders. *Cell* 2000;103:295-309.
- Sakaki-Yumoto M, Katsuno Y, Derynck R. TGF-β family signaling in stem cells. Biochimica et Biophysica Acta (BBA) - General Subjects 2013:1830:2280-96.
- 27. Huang SS, Huang JS. TGF-beta control of cell proliferation. *J Cell Biochem* 2005;**96**:447-62.
- Watabe T, Miyazono K. Roles of TGF-β family signaling in stem cell renewal and differentiation. Cell Res 2008;19:103.
- Ogawa T, Akazawa T, Tabata Y. In vitro proliferation and Chondrogenic differentiation of rat bone marrow stem cells cultured with gelatin hydrogel microspheres for TGF-β1 release. *J Biomater Sci Polym Ed* 2010;21:609-21.
- Li W-J, Tuli R, Okafor C, Derfoul A, Danielson KG, Hall DJ, et al. A three-dimensional nanofibrous scaffold for cartilage tissue engineering using human mesenchymal stem cells. *Biomaterials* 2005;26:599-609.
- Labour M-N, Riffault M, Christensen ST, Hoey DA. TGFβ1 induced recruitment of human bone mesenchymal stem cells is mediated by the primary cilium in a SMAD3-dependent manner. Sci Rep 2016;635542.
- 32. Li D, Liu Q, Qi L, Dai X, Liu H, Wang Y. Low levels of TGF-betal enhance human umbilical cord-derived mesenchymal stem cell fibronectin production and extend survival time in a rat model of lipopolysaccharide-induced acute lung injury. *Mol Med Rep* 2016;14:1681-92.
- Gong Z, Niklason LE. Small-diameter human vessel wall engineered from bone marrow-derived mesenchymal stem cells (hMSCs). FASEB J 2008;22:1635-48.

- Xu Y, James AW, Longaker MT. Transforming growth factor-β1 stimulates Chondrogenic differentiation of Posterofrontal suture–derived mesenchymal cells in vitro. *Plast Reconstr Surg* 2008;122:1649-59.
- 35. Weinreb M, Shinar D, Rodan GA. Different pattern of alkaline phosphatase, osteopontin, and osteocalcin expression in developing rat bone visualized by in situ hybridization. *Journal of bone and mineral research: the official journal of the American Society for Bone and Mineral Research* 1990;**5**:831-42.
- Birmingham E, Niebur GL, McHugh PE, Shaw G, Barry FP, McNamara LM. Osteogenic differentiation of mesenchymal stem cells is regulated by osteocyte and osteoblast cells in a simplified bone niche. *Eur Cell Mater* 2012;23:13-27.
- Komori T. Regulation of Osteoblast Differentiation by Runx2. Boston, MA: Springer US; 201043-9.
- Tang Y, Wu X, Lei W, Pang L, Wan C, Shi Z, et al. TGF-β1-induced migration of bone mesenchymal stem cells couples bone resorption and formation. *Nat Med* 2009;15:757-65.
- Zhao L, Jiang S, Hantash BM. Transforming growth factor beta1 induces osteogenic differentiation of murine bone marrow stromal cells. *Tissue* Eng Part A 2010;16:725-33.
- Lieb E, Milz S, Vogel T, Hacker M, Dauner M, Schulz MB. Effects of transforming growth factor beta1 on bonelike tissue formation in threedimensional cell culture. I. Culture conditions and tissue formation. *Tissue Eng* 2004;10:1399-413.
- 41. Liu P, Oyajobi BO, Russell RG, Scutt A. Regulation of osteogenic differentiation of human bone marrow stromal cells: interaction between transforming growth factor-beta and 1,25(OH)(2) vitamin D(3) in vitro. *Calcif Tissue Int* 1999;65:173-80.
- 42. Jian H, Shen X, Liu I, Semenov M, He X, Wang X-F. Smad3-dependent nuclear translocation of β-catenin is required for TGF-β1-induced proliferation of bone marrow-derived adult human mesenchymal stem cells. *Genes Dev* 2006;**20**:666-74.
- Park J, Kim IY, Patel M, Moon HJ, Hwang SJ, Jeong B. 2D and 3D hybrid Systems for Enhancement of Chondrogenic differentiation of tonsil-derived mesenchymal stem cells. *Adv Funct Mater* 2015;25:2573-82.
- 44. Bi W, Deng JM, Zhang Z, Behringer RR, de Crombrugghe B. Sox9 is required for cartilage formation. *Nat Genet* 1999;**22**:85-9.